Available online at www.sciencedirect.com

ScienceDirect

Mendeleev Commun., 2019, **29**, 355–357

Mendeleev Communications

Synthesis of tungsten nanopowders and modes of their combustion and passivation

Michail I. Alymov,[a] Nikolai M. Rubtsov,*[a] Boris S. Seplyarskii,[a] Victor A. Zelensky[a] and Alexey B. Ankudinov[b]

[a] *A. G. Merzhanov Institute of Structural Macrokinetics and Materials Science, Russian Academy of Sciences, 142432 Chernogolovka, Moscow Region, Russian Federation. Fax: +7 495 962 8025; e-mail: nmrubtss@mail.ru*

[b] *A. A. Baikov Institute of Metallurgy and Materials Science, Russian Academy of Sciences, 119991 Moscow, Russian Federation*

DOI: 10.1016/j.mencom.2019.05.039

Tungsten nanopowders were synthesized by a chemical metallurgy method at 440–640 °C from WO_3 precursors possessing different specific surfaces. The α-W nanopowder synthesized at 640 °C was not pyrophoric, while the α-W containing the traces of oxides obtained at 480 °C was pyrophoric. The temperature interval for the α-W synthesis was revealed as very narrow, from 470 to 490 °C.

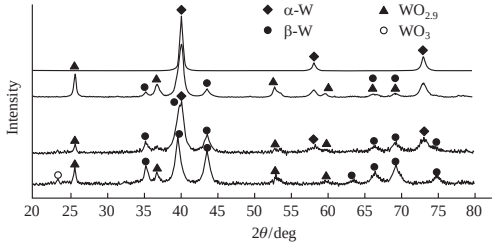

Tungsten-based nanomaterials are useful as direct heated cathode or heater coils for indirectly heated cathodes in cathode ray tubes, magnetrons for microwave ovens, and other devices. The attractive combination of vapor pressure, electrical conductivity, and electronic properties make these nanomaterial compositions suitable substrates for high voltage breakers, incandescent and reflector lamps, fiber-optical systems, video camera lights, medical and scientific instruments, *etc*. The nanomaterials offer several benefits as electron emitters since the nanoparticles can enable the formation of very thin film devices, lower the sintering temperatures and times, exhibit inherently low vapor pressure even at high temperatures, and possess unusual quantum confinement and grain boundary effects. Commonly used photocopiers, laser printers, *etc*. can benefit from charger wires prepared from tungsten comprising nanomaterials. Nanodevices employed in chemical and biomedical sensors, phosphors, and anti-static coatings can be prepared from nanoscale powders comprising tungsten.

Freshly prepared metal nanopowders, in particular, nickel ones, are known as pyrophoric. They self-ignite upon contact with air due to the high chemical activity and large specific surface. To make them safe for a further processing, the powders are passivated *via* the creation of a protective thin oxide film on the surface of nanoparticles.[1]

The stable crystal structure of tungsten (α-W) is body centered cubic. A metastable form (α-W) possesses the A-15 cubic crystal structure containing eight atoms per unit cell.[2] The β-W exhibits a giant spin Hall effect, which makes this material promising for the spintronics aimed at the intrinsic spin of the electron and its associated magnetic moment both in its fundamental electronic charge and solid-state devices.[3] It is considered as a new paradigm for the replacement of conventional charge-based electronics due to the advantages of non-volatility, low power consumption, and high integration density.[4] Spintronics relies on the transport properties of spin polarized current,[3] which is conventionally generated by passing a charge current through a ferromagnetic contact.[5] Nowadays, the spin Hall effect is regarded as a promising mechanism for the generation of spin-polarized current without using any magnetic field or ferromagnetic materials.[6] The β-W is among the materials possessing the highest efficiency in converting the electric current into a spin current,[7] hence it has been adopted as the prototype in the design of spintronic devices.[7,8]

Although β-W has been discovered more than 60 years ago,[9] there are still no definite conclusions about its nature and mechanism of formation. The formation of β-W strongly depends on the deposition parameters, such as the thickness of the films, pressure of inert gas, and presence of oxygen impurity,[7,8] however empirical models, which could quantitatively describe these relationships, have not been developed yet. In particular, the role of oxygen impurity is still under debate: some researchers suggested that β-W should be a non-stoichiometric oxide with the formula of W_3O,[9] while others showed the oxygen element in β-W films to be in a zero valence state, indicating that β-W should be an allotrope of α-W.[10]

The present work was aimed at the establishment of both combustion modes and regimes of passivation of tungsten nanopowders and at the regimes of their synthesis by a chemical metallurgy method in order to determine temperature intervals of the α-W and β-W formation. A partial characterization of the synthesized nanopowders was also performed.

The nanopowders obtained at 480 °C from all the three precursors† were pyrophoric. The self-ignition and combustion

† Three precursors of WO_3 with a different specific surface were used: 2 m^2 g^{-1} (**1**, ISMAN), 11 m^2 g^{-1} (**2**, Novosibirsk, http://raremetal.rf), and 0.8 m^2 g^{-1} (**3**, UK, code B1188). The reactor (Figure S1, Online Supplementary Materials) containing a WO_3 sample in a quartz trough 2 mm thick was maintained in the furnace at 440–640 °C for 2–5 h under hydrogen flow; the reactor was then extracted from the furnace and cooled to room temperature under argon flow. The quartz trough was equipped with a chromel-alumel thermocouple (0.3 mm) placed in the nanopowder. The thermocouple did not touch the walls of the trough. In a number of experiments, the reactor after synthesis and cooling down to

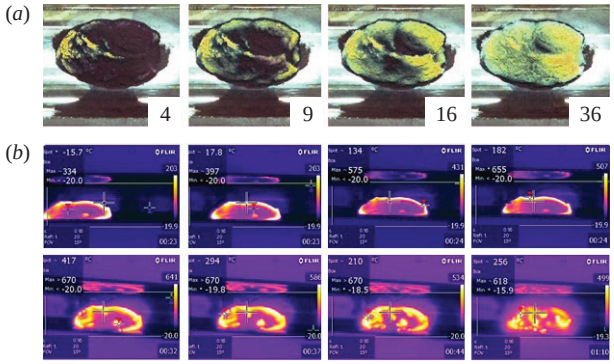

Figure 1 (*a*) Combustion of the nanopowder obtained from the precursor **1** at 480 °C. At the bottom of each frame (right corner), the time (s) after extraction of the trough from the reactor is shown. Initial temperature was 20 °C. (*b*) IR investigation of combustion in the air of the sample obtained from **2** at 480 °C. Initial temperature was 20 °C. At the bottom of each frame (right corner), the time (min : s) after turning on the video camera is shown. The real values of the maximum and minimum temperature are shown near to the left boundary of each frame. A larger cross on the each frame specifies the selected point, where the temperature was recorded; while the smaller cross marked red automatically specifies the point of maximum temperature in the frame.

in the air (precursor **1**, layer thickness of 2 mm) and the IR investigation of its initiated combustion in air are shown in Figure 1. Apparently, the flame front starts from the edge of the sample and propagates to its center; the maximum temperature exceeds 670 °C. The nanopowders obtained from precursors **2** and **3** burned in the same way. During visual data analysis of IR video filming, it is necessary to consider the features of image processing by the used infrared camera:‡ the area with the maximum value of temperature has similar brightness for all frames at the given moment.

The α-W nanopowders obtained at 640 °C from the three precursors did not self-ignite (*i.e.*, were not pyrophoric) but could be ignited with a heated wire. Figure 2(*a*) demonstrates a finger-like character of initiated combustion in the case of α-W nanopowder. The local self-heating at the center of a sample extracted from the reactor immediately after synthesis [Figure 2(*b*), two left frames] did not lead to a propagation of the flame front, but after cooling, either sample of the nanopowder could be ignited with a heated wire [see Figure 2(*b*), two right frames]. Thus, the

room temperature was placed in an external bath of a HAAKE-Q cryostat, where it was cooled (0 to –35 °C) under argon flow (EtOH was a cooling agent).[12] Upon reaching the necessary subzero temperature, Ar flow was replaced by the dry air flow to passivate the nanopowder. To dry the air used, it was passed through a column of solid alkali (KOH) 0.6 m long and then through the coil of a flexible tubing placed in the cooled bath of the cryostat. The detected heating of the thermocouple after replacing flows indicated the beginning of the ignition. If the ignition occurred, the surface of a sample changed its color from black to yellow (WO_3 is green-yellow). If the ignition was not started in 30 min, the air flow was replaced with the argon flow and the reactor was heated up to room temperature. Then the quartz trough with the passivated nanopowder was extracted from the reactor, and the nanopowder was immediately placed on Ni foil to avoid spontaneous ignition. The nanopowder was then placed on the sample stage for high-speed video recording. The withdrawal of the trough and placing it on the stage took about 5 s. In another series of experiments, the passivation of the nanopowder was performed at 20 °C for 1 h in the mixed flow of air (3%) and Ar.

‡ Nicon 1 (30 fps) color video and Flir 60 (30 fps, 320×240 pix, sensitivity interval of 8–14 μm) infrared cameras were used to establish the combustion modes. Phase composition of the obtained samples was investigated by a DRON 3M X-ray diffractometer equipped with a coordinate-sensitive detector. The measurement of the specific surface values was performed using a Sorbi-M analyzer by the BET method.

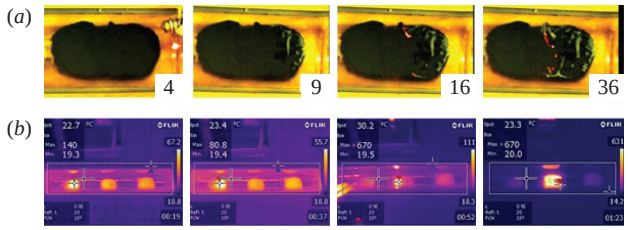

Figure 2 (*a*) Initiated combustion in the air of α-W nanopowder obtained at 640 °C from precursor **1**. The time (s) after initiation with a heated wire is shown at the bottom right corner. (*b*) IR investigation of the warming-up under air of α-W nanopowders of different thickness (precursor **1**; 1, 2 and 3 mm from left to right) obtained at 640 °C. The two right frames show initiated combustion of the sample 2 mm thick. At the bottom of each frame to the right, the time (min : s) after initiation is shown. Initial temperature was 20 °C.

maximum temperature for the burning sample in a 'tip' of the 'finger' exceeds 670 °C.

Time dependences for the warming-up of the nanopowder (obtained at 480 °C from precursor **1**) during its passivation in the flow of dry air at initial temperatures –34, –30 and –24 °C are shown in Figure 3, where the zero time corresponds to the moment of replacing Ar flow with the passivating dry air flow. The maximum warming up at the initial temperature of passivation –24 °C was until 170 °C, after that the sample color changed to yellow. For the passivation temperatures of –30 and –35 °C, the maximum warming up values were ~20 and ~0 °C, respectively.

If the ignition was not started within 30 min (*i.e.*, the sample did not change its color), the air flow was replaced with Ar one, and the reactor was heated to room temperature. The quartz trough with the passivated nanopowder was then extracted from the reactor. However, as distinct from iron, nickel and copper nanopowders,[12–14] the processing of the obtained nanopowders did not ensure their passivation since the sample self-ignited upon its contact with air. The ignition of nanopowder could be avoided if it was placed on a Ni foil immediately after the extraction. Thus, the passivation at subzero temperatures was ineffective without providing additional heat losses to the metallic foil. Therefore, the passivation was mainly performed at room temperature for 1 h under the mixed air (3%) and argon flow. This procedure prevented self-ignition of the nanopowder in the air.

BET surface areas for the nanopowders obtained from all three precursors at 480 (passivated) and 640 °C (nonpassivated), were 15±3 and 9±2 $m^2\ g^{-1}$, respectively.

The X-ray phase analysis (Figure 4) of the nanopowders obtained at 640 °C from precursors **1**–**3** revealed that the samples contained only α-W [Figure 4(*a*)], while the samples of passivated tungsten nanopowders obtained at 500 °C from precursors **1**–**3** contained α-W, β-W, and $WO_{2.9}$ [Figure 4(*b*)]. The sample of passivated tungsten nanopowder obtained at 480 °C from precursor **3** contained only β-W and traces of tungsten oxides [Figure 4(*d*)]. The tem-

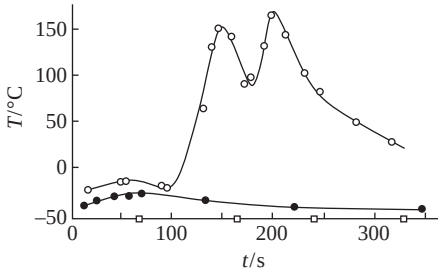

Figure 3 Time dependence of the warming up of the sample obtained from precursor **1** during passivation under the dry air flow at (○) –24, (●) –30 and (□) –34 °C.

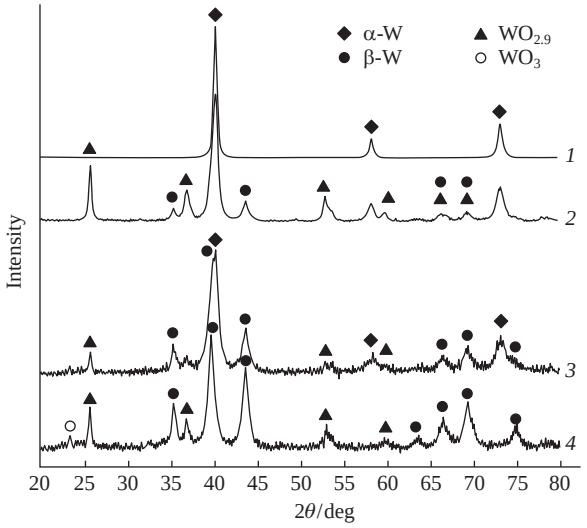

Figure 4 X-ray phase analysis at the initial temperature of 20 °C for (*1*) the passivated tungsten nanopowder obtained at 640 °C from precursor **1**, (*2*) at 500 °C from **2**, (*3*) at 480 °C from **2** and (*4*) at 480 °C from **3**.

perature interval for α-W synthesis was found being very narrow: 470–490 °C, although in another report,[2] the optimum temperature was 500 °C. The presence of traces is evidently due to the passivation procedure. The X-ray spectrum of the product obtained from presursor **2** at 480 °C, which was the mixture of α-W, β-W, WO_3, and $WO_{2.9}$, is also shown for comparison [Figure 4(*c*)]. At reduction temperatures between 500 and 650 °C, the product was a mixture of β-W and α-W, while the amount of α-W increased with raising the temperature. Above 640 °C, only α-W was obtained.

Previously,[2] it was concluded that an X-ray pure β-W product is obtained if the specific surface of initial WO_3 is more than 4.65 m^2 g^{-1}. If the precursor with that of 1.07 m^2 g^{-1} was used, only mixtures of α-W with $WO_{2.9}$ were produced. In the present work, the β-W was obtained from WO_3 precursor with the specific surface of 0.8 m^2 g^{-1}, while the WO_3 precursor with that of 11 m^2 g^{-1} led to the mixture of α-W, β-W, and $WO_{2.9}$. Therefore, our results suggest that the value of specific surface does not affect the yield of β-W.

In conclusion, the tungsten nanopowders were synthesized *via* the hydrogen reduction method at 440–640 °C from the WO_3 precursors possessing the different specific surface: 2 (**1**), 11 (**2**), and 0.8 m^2 g^{-1} (**3**). It has been shown that the nanopowder prepared at 640 °C from precursors **1**–**3** is the α-W and not pyrophoric. Its combustion can be initiated by an external source, and the combustion is developing in the finger-like mode. The nanopowder obtained at 480 °C from precursors **1** and **2** is the mixture of α-W, β-W, and $WO_{2.9}$, and it is pyrophoric due to the presence of β-W. The nanopowder synthesized at 480 °C from precursor **3** is the β-W containing only traces of WO_3 and $WO_{2.9}$. The temperature interval suitable for the α-W synthesis was very narrow (470–490 °C). The α-W and passivated β-W nanopowders possess the specific surface of 10±2 and 18±1 m^2 g^{-1}, respectively. The dynamics of temperature fields during the ignition and combustion of tungsten nanopowders has been characterized.

This work was supported by the Russian Science Foundation (grant no. 16-13-00013).

Online Supplementary Materials

Supplementary data associated with this article can be found in the online version at doi: 10.1016/j.mencom.2019.05.039.

References

1 A. G. Gnedovets, A. B. Ankudinov, V. A. Zelenskii, E. P. Kovalev, H. Wisniewska-Weinert and M. I. Alymov, *Inorg. Mater: Appl. Res*., 2016, **7**, 303 (*Persp. Mater*., 2015, 62).
2 W. R. Morcom W. L. Worrell H. G. Sell and H. I. Kaplan, *Metall. Trans*., 1974, **5**, 155.
3 I. Žutić, J. Fabian and S. Das Sarma, *Rev. Mod. Phys*., 2004, **76**, 323.
4 S. A. Wolf, D. D. Awschalom, R. A. Buhrman, J. M. Daughton, S. von Molnár, M. L. Roukes, A. Y. Chtchelkanova and D. M. Treger, *Science*, 2001, **294**, 1488.
5 M. Johnson and R. H. Silsbee, *Phys. Rev. Lett*., 1985, **55**, 1790.
6 T. Jungwirth, J. Wunderlich and K. Olejnik, *Nat. Mater*., 2012, **11**, 382.
7 C.-F. Pai, L. Liu, Y. Li, H.-W. Tseng, D. C. Ralph and R. A. Buhrman, *Appl. Phys. Lett*., 2012, **101**, 122404.
8 Q. Hao, W. Chen and G. Xiao, *Appl. Phys. Lett*., 2015, **106**, 182403.
9 G. Hägg and N. Schönberg, *Acta Crystallogr*., 1954, **7**, 351.
10 P. Petroff, T. T. Sheng, A. K. Sinha, G. A. Rozgonyi and F. B. Alexander, *J. Appl. Phys*., 1973, **44**, 2545.
11 E. Lassner and W.-D. Schubert, *Tungsten: Properties, Chemistry, Technology of the Element, Alloys, and Chemical Compounds*, Kluwer Academic / Plenum Publishers, New York, 1998.
12 M. I. Alymov, N. M. Rubtsov, B. S. Seplyarskii, V. A. Zelensky and A. B. Ankudinov, *Mendeleev Commun*., 2017, **27**, 482.
13 M. I. Alymov, N. M. Rubtsov, B. S. Seplyarskii, V. A. Zelensky, A. B. Ankudinov, G. I. Tsvetkov and V. I. Chernysh, *Mendeleev Commun*., 2018, **28**, 447.
14 M. I. Alymov, N. M. Rubtsov, B. S. Seplyarskii, R. A. Kochetkov, V. A. Zelensky and A. B. Ankudinov, *Mendeleev Commun*., 2017, **27**, 631.

Received: 5th October 2018; Com. 18/5712